

Mild steel corrosion inhibition by some heteroatom organic compounds in acetic acid medium

A. Bouchtart^(a), M. Rguiti^(b), K. EL Mouaden^(a), A. Albourine^{(a)*}, A. Chaouiki^(c), R. Salghi^(c), L. Bazzi^(b), A. Chetouani^(d)

^(a) Team of Chemistry Physic, Faculty of Sciences, Ibn Zohr University, Agadir, Morocco

^(b) Analytical Chemistry and Environment Team, Materials and Environment Laboratory, Faculty of Sciences Ibn Zohr University Agadir Morocco

^(c) Team of Applied Chemistry and Environment, ENSA, University Ibn Zohr, Box: 1136, Agadir, Morocco

^(d) Laboratoire de Chimie Analytique Appliquée, Matériaux et Environnement (LC2AME) Faculté des Sciences Oujda Morocco.

Abstract

Four heteroatom organic compounds (HAC) such as L-methionine (Meth), L-Cysteine (Syst), Phenyl MercaptoTetrazol (PMT) and Glutamic acid (GA) were evaluated as corrosion inhibitors for mild steel in 1M acetic acid (AcA) solution. The technique used are potentiodynamic polarization (PDP), electrochemical impedance spectroscopy (EIS), UV-Vis spectroscopy analysis and scanning electron microscopy (SEM). As a comparative study results, the corrosion inhibitor rankings were: Meth < Cyst < PMT < GA. Furthermore, the GA was the best inhibitors against mild steel corrosion and provided an inhibition efficiency of 74% at 10⁻⁴M. For this reason, we have besides studied the GA concentration and immersion time on the performance delivered by GA. In this way, it is affirmed that the inhibition efficiency was well improved with the GA concentration increasing. In addition, the GA is a good corrosion inhibitor even with long durations.

* Corresponding author:

albourine@yahoo.fr

Received 22 April 2020,

Revised 10 sept 2020,

Accepted 22 sept 2020

Keywords: heteroatom organic compounds, corrosion, inhibition, Mild Steel, Acetic Acid.

1. Introduction

Mild steel is one of the most used steel types in industrial fields. This large application is due to its low cost and high strength. However, the mild steel provides a limited properties and applications in many aggressive environments due to corrosion attack. This deterioration is more announced in acidic media (acid cleaning, descaling, and drilling operations in oil and gas exploration) joined to other several conditions. In fact, the reduction of the free energy value is a fundamental reason of the steel corrosion problems. All previous details make the mild steel a sensible material to corrosion phenomenon. In recent years, a number of amino acids are exploited as eco-friendly corrosion inhibitors and as an environmentally alternative to hazardous and toxic compounds that are widely used to limit material deteriorations. These organic compounds containing N, O and S atoms are considered to be effective corrosion inhibitors and environmentally respected additives [1]. For example, L-lysine acted as a mixed-type inhibitor in HCl solution and a modest cathodic inhibitor in H₂SO₄ against mild steel corrosion. It was affirmed that the synergetic effect of chloride ions reinforced the corrosion inhibition of L-lysine in H₂SO₄ medium[2]. While, the inhibitory effect of L-leucine and trypsin was announced when they are mixed in dilute sulphuric acid [3]. On the other hand, the Glutamic acid was tested as a corrosion inhibitor for carbon steel in seawater and a formula of 200 ppm of Glutamic acid and 20 ppm of Zn²⁺ has 87% of inhibition efficiency [4]. In addition, the L-tryptophan exhibited good performance as corrosion inhibitor in HCl for mild steel. This performance was improved with the addition of the surfactants [5]. An examination of a literature indicates that the most amino acids are not enough tested on the organic acids as the aggressive medium. For this purpose, in the present work, we are interested to investigate the effect of some amino acids namely GA, Cyst and Meth on the corrosion behavior of mild steel in acetic acid (AcA) as an organic medium. For comparison, we tested in the same medium the effect of PMT as a potential corrosion inhibitor in other corrosive solutions [6,7].

2. Materials and methods

2.1. Material and electrolyte

The 1M acetic acid was prepared using analytical grade acetic acid with distilled water. Glutamic acid (GA), phenyl mercaptotetrazol (PMT), Cysteine (Cyst) and L-methionine (Meth) were purchased from Aldrich® with 99 % of purity. The tested mild steel samples have a chemical composition (in Wt %) of 0.179 % C, 0.165 % Si, 0.439 % Mn, 0.203 % Cu, 0.034 % S and balance Fe, with an exposed surface area about 0.3 cm². All the experiments are carried out at a constant temperature of 25 ± 0.1 °C.

2.2. Electrochemical measurements details

All the electrochemical measurements are carried out in corrosion cell with calomel electrode (saturated KCl) as reference electrode, Pt as counter electrode and steel-based electrode as working electrode (WE). Before each test, the working electrode was polished mechanically with an emery paper of 1200 grade, washed with acetone and with double distilled water, then transferred immediately to electrochemical cell with the tested electrolyte. For testing the inhibitive ability of the different tested HAC, potentiodynamic polarization (PDP) and electrochemical impedance spectroscopy (EIS) are explored using a VoltaLab® LG304 potentiostat/galvanostat with VoltaMaster 4 as control software. At first, the WE is maintained at its open circuit potential for 30 min. The EIS measurements were performed using AC signals of amplitude 10 mV peak-to-peak at the OCP in frequency range from 100 kHz to 10 mHz. On the other hand, the polarization curve is achieved in potential range from cathodic to anodic potentials with a scan rate of 30 mV/min. the inhibition efficiency obtained from the two used electrochemical methods was calculated as follows:

$$E_i \% = \left(\frac{i_{\text{corr}}^0 - i_{\text{corr}}}{i_{\text{corr}}^0} \right) \times 100 \quad (1)$$

$$E_z \% = \left(\frac{R_{\text{ct}} - R_{\text{ct}}^0}{R_{\text{ct}}} \right) \times 100 \quad (2)$$

Where i_{corr}^0 , i_{corr} , R_{ct}^0 and R_{ct} present the corrosion current densities and charge transfer resistance without and with inhibitor, respectively.

2.3. Weight loss tests

In order to estimate the corrosion rate of mild steel in acetic acid medium in the absence and presence of the tested inhibitor, the weight loss measurements are carried out using Shimadzu, UV mini-1240 Spectrophotometer analysis. For this reason, mild steel coupons of dimensions of 1.5 x 2 x 0.001 cm were mechanically polished by different grit SiC papers, washed with double distilled and degreased using acetone, and dried up. After what, the samples are immersed in 200 ml of different tested solutions (without and with inhibitor) for different periods until 480 hours. For each immersion period, a volume of 10 ml is taken from each solution to realize the weight loss measurements and induce the corresponding corrosion rate (V_{corr}) and inhibition efficiency (E_G) using the following equations:

$$V_{\text{corr}} = \frac{\Delta m}{S \cdot t} \quad (3)$$

$$E_G \% = \left(\frac{V_{\text{corr}}^0 - V_{\text{corr}}}{V_{\text{corr}}^0} \right) \times 100 \quad (4)$$

Where V_{corr}^0 , V_{corr} , Δm , S and t present the corrosion rate without and with inhibitor, weight loss value, surface working electrode and immersion time, respectively.

2.4. Surface analysis

The morphology of the surface of mild steel was observed with a scanning electron microscope SEM (Jeol JSM-6460LAV) operating at 15 kV. All the samples are observed by SEM after polishing and after an immersion time of 480 hours in uninhibited and inhibited acidic medium.

2.5. Theoretical calculations

In order to gain further insight into the reactivity of the studied inhibitor molecule, quantum chemical calculations were performed by using reliable module implemented in the high-performance software (Materials Studio version 6.0)[8]. Also, in this way, to provide a detailed theoretical explanation to the experimental results, other parameters based on Fukui functions were calculated to identify and better understanding active sites on the structural geometry of the molecule. All the calculations obtained throughout this method were performed using generalized gradient approximation (GGA) and Perdew, Burke and Ernzerhof formalism known as PBE with "double-numeric plus polarization" (DNP) basis set and the COSMO implicit solvent model [9–11]. The Glutamic acid was thoroughly analyzed, and the optimized structure is used to estimate some useful derived parameters. By these calculations, the frontier molecular orbitals such as the energy of the highest occupied molecular orbital (E_{HOMO}) and energy of lowest unoccupied molecular orbital (E_{LUMO}) were calculated by applying the Koopmans' theorem[12,13]. The ionization energy (IE), the electronic affinity (EA) and energy gap ΔE were determined by the values of the energies of the

HOMO and LUMO orbitals and from which, the electronegativity and the global hardness of the extracted molecule were calculated[14].

$$IE = -E_{\text{HOMO}} \quad (5)$$

$$EA = -E_{\text{LUMO}} \quad (6)$$

$$\text{Absolute electronegativity } (\chi) \chi = \frac{IE + EA}{2} \quad (7)$$

$$\text{Absolute hardness } (\eta) \quad \eta = \frac{IE - EA}{2} \quad (8)$$

$$\Delta E = E_{\text{LUMO}} - E_{\text{HOMO}} \quad (9)$$

Moreover, the number of transferred electrons (ΔN) is calculated by application of the Pearson method using the following equation[15]:

$$\Delta N = \frac{\phi - \chi_{\text{inh}}}{2(\eta_{\text{Fe}} + \eta_{\text{inh}})} \quad (10)$$

The work function (ϕ) of the Fe(110) was generally known to be 4.82 eV while the absolute hardness η_{Fe} of iron was estimated as 0 since $I = A$ for bulk metals [13,16,17].

To investigate the electronic properties of the studied molecule, the condensed Fukui functions were estimated based on a Hirschfeld Population Analysis (HPA) with same setting parameters mentioned above and the finite difference approximation as follows[13,16,18]:

$$f_k^+ = q_k(N+1) - q_k(N) \quad \text{For nucleophilic attack} \quad (11)$$

$$f_k^- = q_k(N) - q_k(N-1) \quad \text{For electrophilic attack} \quad (12)$$

Here, as elements listed in the above equations; q_k is the electronic population of an atomic site within a molecule in its neutral (N), anionic (N+1) or cationic (N-1) state.

3. Results and discussion

3.1. Corrosion inhibition

Fig. 1 illustrates the addition effect of 10^{-4} mol/L of different HAC namely Glutamic acid, PMT, Cysteine and L-methionine on the Nyquist plots 25 ± 0.1 °C. In order to evaluate the inhibitory efficiency ($E_{\%}$) against steel corrosion of each tested inhibitor, it is estimated using the following equation:

$$E_{\%} = \left(\frac{R_{ct}^0 - R_{ct}}{R_{ct}^0} \right) \times 100 \quad (13)$$

Where R_{ct}^0 and R_{ct} present the charge transfer resistance without and with inhibitor, respectively.

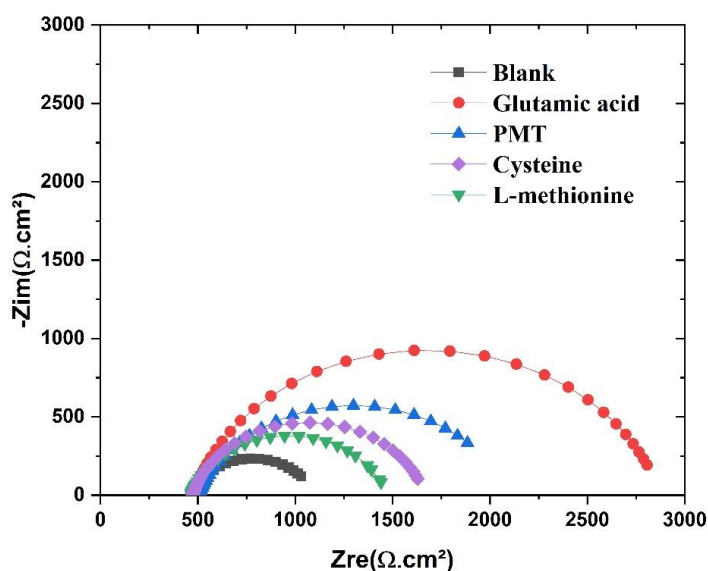


Fig. 1: Impedance diagrams obtained for mild steel in 1M AcA, in absence (Blank) and presence of 10^{-4} mol/L of the studied amino acids.

It is obvious that all the Nyquist diagrams can be characterized by a single capacitive loop with a corresponding diameter depending on the kind of the tested HAC. It can be concluded that the addition of HAC did not have significant influence on the corrosion behavior. The existence of one capacitive loop in Nyquist plot confirms that the electrode-solution interface is controlled by the electron transfer reaction[19]. Therefore, it is attributed to the dissolution of the iron in acidic medium [20]. The impedance parameters of the obtained plots for mild steel immersed in AcA (1M) are adjusted and calculated using the equivalent electric circuit represented in Fig. 2. As the circuit shown, R_s refers to the solution resistance, R_{ct} is the charge transfer resistance and the CPE_{dl} denotes the constant phase element and is related to the capacitance of the double layer. The CPE is generally used instead of the double layer capacity due to the deviation recorded from the ideal capacitor. In fact, the use of CPE permits to compensate the deviation of the ideal dielectric behavior related to the inhomogeneous electrode surface [21, 22]. Moreover, the CPE impedance (Z_{CPE}) can be expressed using the following equation [23-25]:

$$Z_{CPE} = Y_0^{-1}(j\omega)^{-n} \quad (14)$$

Where, Y_0 is a proportionality coefficient, ω denotes the angular frequency (having units in rad sec^{-1}), and n denotes the phase shift.

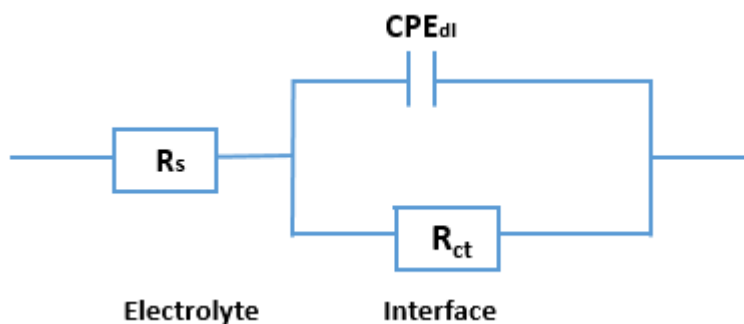


Fig. 2: The equivalent electric circuits used to fit the experimental impedance data obtained for mild steel in AcA medium without and with different added amino acids.

From the Table 1, we observed that for all the amino acids, the increase of R_{ct} is accompanied with a significant decrease at the CPE_{dl} value and, correspondingly, the inhibition efficiency rise. It was found that GA provided the best inhibitory efficiency with a higher charge transfer resistance of 2400 Ohm.cm² responsible for 73.68 % of inhibition efficiency. On the other hand, the lower corrosion inhibition was attributed to L-methionine (37.40 %). In addition, the inhibition efficiency obeys the following order: Glutamic acid > PMT > Cysteine > L-methionine. This behavior can be attributed to the variation of number and type of hetero-atoms containing in the inhibitor structure namely N, O and S [26]. For this reason, in the second section, we are interested in investigating the effect of GA concentration and immersion time on the inhibition efficiency against mild steel corrosion in 1M AcA.

Table 1: The EIS parameters for mild steel in AcA solution without and with 10⁻⁴ mol/L of different amino acids at 25 ± 0.1 °C.

	R_s (Ohm.cm ²)	CPE_{dl} (μF.cm ⁻²)	R_{ct} (Ohm.cm ²)	E_z (%)
Blank	464.10	57.50	631.70	-
L-methionine	465.34	20.01	1009.00	37.40
Cysteine	467.73	17.24	1194.00	47.09
PMT	501.00	16.20	1590.00	60.30
Glutamic acid	475.50	7.84	2400.00	73.68

3.2. Influence of concentration on the performance of GA

3.2.1. Potentiodynamic polarization

In this section, we have tested the influence of the concentration of GA on the corrosion of mild steel in 1M AcA. The obtained results are represented in Fig. 3. First of all, we noticed that cathodic and anodic regions and their corresponding kinetics are not affected by the addition of different concentrations of GA. Moreover, the tafel curves, in the presence of GA, showed a shift of the corrosion potential to more negative value compared with the uninhibited acidic medium. On the other hand, the corrosion current density decreases with the increase of GA concentration. In order to yield a quantitative approach, the I_{corr} , E_{corr} , anodic and cathodic Tafel slopes are evaluated from the experimental data. To estimate the inhibition efficiency of the GA against mild steel corrosion, we are using the following equation:

$$E_{PDP} \% = \left(\frac{i_{corr}^0 - i_{corr}}{i_{corr}^0} \right) \times 100 \quad (15)$$

Where i_{corr}^0 and i_{corr} present the corrosion current density without and with inhibitor, respectively. All the determined parameters are summarized in the Table 2. We remarked that the corrosion current density decreases and the corresponding inhibition efficiency increases considerably when the GA concentration is augmented at the acidic medium. This result confirmed that the GA molecules were adsorbed on the mild steel surface at acidic pH and preventing the corrosion effects. On the other hand, we observed that the anodic and cathodic slopes (β_a and β_c) did not significantly change with the GA concentration, which means that the anodic and cathodic reaction mechanism is not affected during the GA concentration augmentation. Briefly, the best corrosion inhibition is provided by 5.10⁻⁴ mol/L of GA (83.40 %).

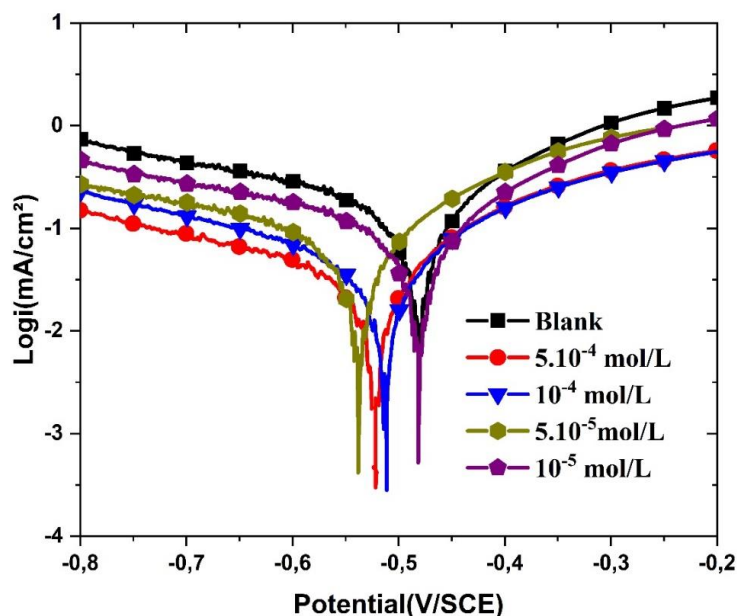


Fig. 3: Potentiodynamic polarization curves of mild steel in 1M AcA in the absence and presence of different concentrations of GA.

Table 2: Data obtained from polarization curves for mild steel in 1M of AcA in the absence and presence of different concentrations of GA.

	$-E_{corr}$ (mV)	I_{corr} ($\mu A/cm^2$)	$-\beta_c$ (mv.dec ⁻¹)	β_a (mv.dec ⁻¹)	E_{PDP} (%)
Blank	483.90	175.00	468.70	220.40	-
1x10⁻⁵ mol/L	481.40	76.64	437.90	227.70	56.15
5x10⁻⁵ mol/L	537.34	63.10	467.10	250.10	63.94
1x10⁻⁴ mol/L	514.12	56.50	435.54	232.20	72.65
5x10⁻⁴ mol/L	522.00	29.06	437.90	227.70	83.40

3.2.2. Electrochemical impedance spectroscopy

In order to confirm and compare the obtained potentiodynamic polarization measurements with others, we are studying the inhibition process using the electrochemical impedance spectroscopy. The Fig. 4 illustrates EIS spectra of mild steel in AcA without and with different concentrations of GA. The diameter of the depressed circle increased with the GA concentration increasing with indicates that the protection ability of the formed film on the mild steel surface rises with the increasing inhibitor concentration [27]. Furthermore, the presence of GA molecules does not affect the whole process at the interface mild steel surface-acidic solution. According to the fitting results in Table 3, the charge transfer resistance increases with the addition of GA despite its concentration. In other words, the minimal concentration of 10^{-5} mol/L is responsible for 56.28 % of the corrosion inhibition efficiency. The last keep to rise with the GA concentration increasing until reaching 80.35 % with $5 \cdot 10^{-4}$ mol/L. In fact, this result can be interpreted by the adsorption of an amount of GA molecules at the steel-acid interface. The thickness of the formed film augmented with the GA concentration and justified by the CPE_{dl} values decrease due to the inhibitor molecules adsorbed at the inner Helmholtz plane and block, thereafter, the active sites on the metallic surface[28].

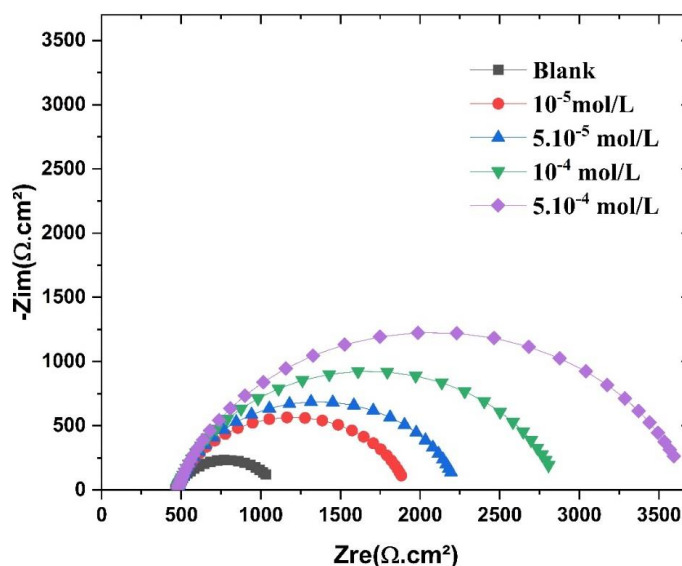


Fig. 4: Nyquist plots obtained for mild steel in 1M of AcA without and with different concentrations of GA.

Table 3: The EIS parameters for mild steel in AcA solution without and with different concentrations of GA at 25 ± 0.1 °C.

	R_s (Ohm.cm ²)	CPE_{dl} (μF.cm ⁻²)	R_{ct} (Ohm.cm ²)	E_z (%)
Blank	464.10	57.50	631.70	
1x10⁻⁵ mol/L	474.40	12.31	1445.00	56.28
5x10⁻⁵ mol/L	474.20	10.28	1767.00	64.25
1x10⁻⁴ mol/L	475.50	7.84	2400.00	73.68
5x10⁻⁴ mol/L	475.20	6.07	3214.00	80.35

3.3. Influence of immersion time on the performance of GA

The corrosion of mild steel in 1M AcA in the absence and presence of varying concentrations of GA was evaluated during a time range from 24 to 480 hours employing weight loss measurement. The Table 4 (Fig. 5) showed the calculated values of corrosion rate and the corresponding inhibition efficiency at a tested concentration of 10^{-4} M of GA. In parallel to the weight loss technique, the scanning electron microscopy is also investigated in order to visualize the effect of acidic medium without and with the GA molecules on the surface of the mild steel. The steel samples are observed using the SEM after immersion for 480 hours. The Fig. 6 (a, b and c) displayed the obtained SEM micrographs. From the obtained data, it is seen that the corrosion rate of the mild steel depends upon two mainly factors namely the addition of GA and the immersion time. Firstly, the corrosion rate increases with the immersion time in the uninhibited acidic medium. This result confirms that the steel surface is not protected and a corrosion rate of $4.39 \mu\text{g/h.cm}^2$ is recorded after a maximum immersion time of 480 hours. This behavior is supported by SEM, which shows a corroded surface (Fig. 6(b)) with compared to the steel surface before immersion (Fig. 6(a)). While, the

corrosion effect is significantly reduced by the addition of AG in the acetic acid medium through decreasing the corrosion rate of the studied steel. However, in the presence of GA, the steel corrosion rate undergoes a slight increase when the immersion time increases but it steels less than the values recorded in uninhibited medium. In fact, the surface immersed in inhibited medium remains intact and no streak of corrosion process is observed (Fig. 6(c)). This observation requires that the molecules of the AG inhibitor act by blocking the surface of the steel by a simple adsorption [4, 28]. On the other hand, the inhibitory efficacy of GA tends to increase when the duration of immersion increases to around 200 hours. For longer immersion times, E_G remains constant with an average value of 70%. This result displays that AG acts effectively in reducing the corrosion process of steel even for long periods of immersion.

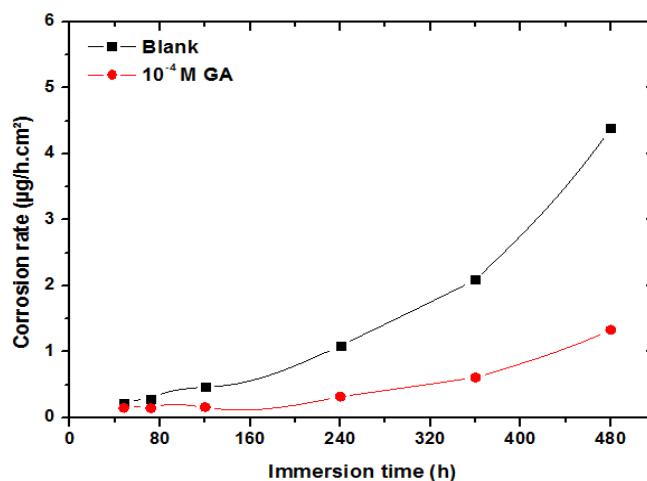
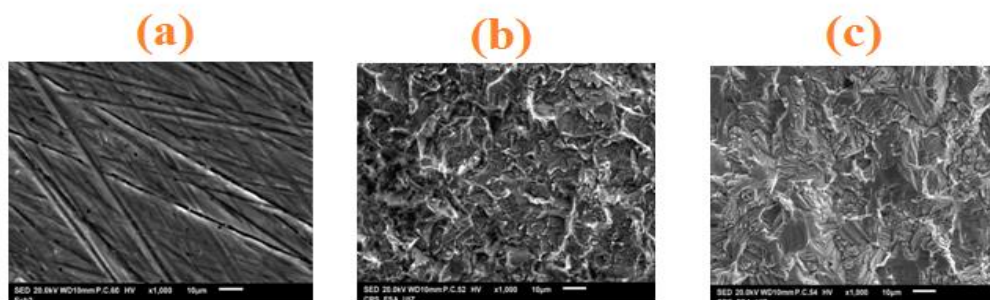


Fig. 5: Plots of corrosion rate (V_{corr}) versus immersion time for mild steel in 1M AcA in the absence and presence of 10^{-4} M of GA.

Table 4: Corrosion parameters for mild steel in 1M AcA in the absence (V_{corr}^0) and presence (V_{corr}) of GA.

Immersion time	V_{corr}^0 ($\mu\text{g/h.cm}^2$)	V_{corr} ($\mu\text{g/h.cm}^2$)	E_G (%)
24	ε	ε	00
48	0.22	0.15	33
72	0.28	0.14	50
120	0.47	0.16	67
240	1.09	0.32	70
360	2.09	0.61	71
480	4.39	1.33	70



3.4. DFT calculations: Global reactivity and Fukui functions

In recent years, researchers have investigated a variety of approaches to evaluate inhibitor-metal interactions and to extract more information related to chemical structure proprieties during the corrosion process by inhibitor compounds. Among them, computational chemistry techniques based on density functional theory calculations have emerged as a powerful tool in studying the behaviour of metal corrosion by inhibitor molecules in terms of inhibition efficiency and its relation to the structure and reactivity of the main components synthesized[16]. Herein, we used this method for analyzing multiple parameters related to the reactivity of Glutamic acid as an efficient inhibitor as explain and interpreted in different experiments used in this study. Fig.7 presents the optimized molecular structures, highest occupied molecular orbital (HOMO) and the lowest unoccupied molecular orbital (LUMO) of Glutamic acid, while some calculated quantum chemical parameters like E_{HOMO} , E_{LUMO} , ΔE_{gap} and ΔN are given in Table5. The term of HOMO energy is generally understood to mean the ability of a compound to offer electrons to another molecule having empty orbits. So, a high value of HOMO energy has come to be used to refer to the good ability of an inhibitor compound to donate electrons to the vacant orbital of the metal atoms[17]. In contrast, a low LUMO energy denotes the high capacity to accept electrons[18]. Moreover, ΔE_{gap} is an important parameter characteristic of electronic molecular proprieties, and plays a key role and helps us to interpret and better understanding the reactivity and stability of corrosion inhibitor molecules[29]. Based on this parameter a greater inhibition effect of an inhibitor molecule is obtained when the ΔE_{gap} value is relatively low [30, 31]. Overall, the most interesting aspect of the graphical representation of HOMO and LUMO orbitals is that the highest electron density is mostly concentrated on the S, O and N atoms. These indicate that the reactivity of these heteroatoms is high which could be responsible for the interaction with Fe atoms.

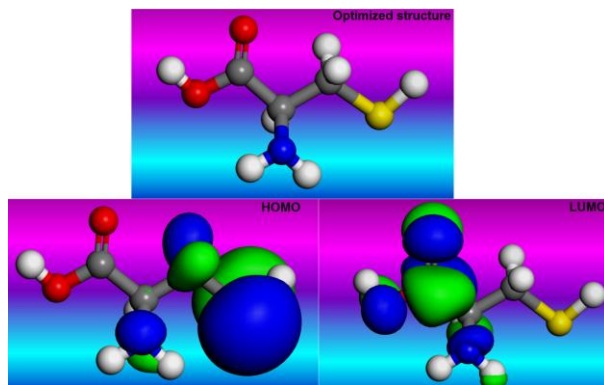


Fig. 7: Optimized molecular structure of Glutamic acid and the electron density distribution of HOMO and LUMO derived using DFT method.

Table 5. The quantum chemical parameters for Glutamic acid analysed from DFT method in aqueous solution.

Molecule	$E_{\text{HOMO}}(\text{eV})$	$E_{\text{LUMO}}(\text{eV})$	$\Delta E_{\text{gap}}(\text{eV})$	$EA(\text{eV})$	$IE(\text{eV})$	$\chi(\text{eV})$	ΔN_{H}
GA	-5.517	-2.918	2.599	5.517	2.918	4.217	0.231

According to the data presented in Table 5, we can infer that the E_{HOMO} is high indicating that it has the highest electron-donating ability to the iron atoms. Moreover, the value of E_{LUMO} showed the electron-accepting tendency of this compound (from metal to inhibitors). In addition, based on the values of ΔE , the reactivity of the GA compound is interesting and therefore the inhibition performance of the GA is high compared with other amino acids tested in the present work. The results of this investigation (Table 5) show also that the calculated value of fraction of electron

transfer (ΔN) is greater than zero confirm that the Glutamic acid has the ability to transfer their electrons to the iron surface[31,32]. So far, the most reactive sites have been identified in order to predict the best adsorption sites for nucleophilic and electrophilic exchanges as being potentially important in the studied molecule that has the ability to improve the corrosion inhibition of mild steel. For this purpose, the condensed Fukui functions of Glutamic acid were estimated to get a better insight into the general reactivity of this compound. In the literature, a high positive charge (f_k^+) of the molecule could be associated with the site favored for a nucleophilic attack, while the site that has high negative charges (f_k^-) could be attributed for an electrophilic attack[33,34]. The condensed Fukui functions (f_k^+ and f_k^-) are graphically shown in Figure 8. From the chart, it can be seen that the S atom has a high tendency of f_k^- meaning that this sit is favored for the electrophilic attack. On the other hand, the most favorable sites for an electrophilic attack f_k^+ are oxygen and nitrogen atoms as well as some atoms of carbon. In general, therefore, it seems that these centers of nucleophilic and electrophilic attacks are in good agreement with the electron density distribution over the HOMO and LUMO orbitals, which provide further support and draw our attention to the importance of considering the Glutamic acid as a good inhibitor due to its high capability to interact the mild steel surface through donor-acceptor interactions.

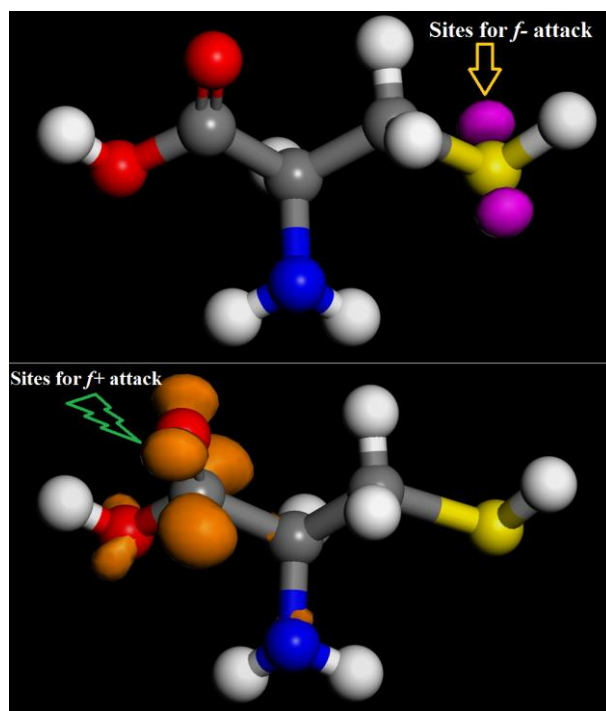


Fig. 8: Graphical representation of the Fukui functions in terms of most reactive sites distribution onto the investigated inhibitor.

4. Conclusion

The current study concerns the evaluation of four HAC as corrosion inhibitor of mild steel in AcA media. All the used methods are in good agreement and leads to the following conclusions: Meth < Cyst < PMT < GA. The GA compound exhibits a good inhibition efficiency of 73.68 % at 10^{-4} M. This efficiency value is improved by increasing in GA concentration arriving at 80.35 % by the concentration of 5.10^{-4} mol/L. this amino acid demonstrates its good ability to protect the mild steel in acidic medium even at long durations. The SEM analysis reveals the formation of a protective film on the steel surface. The quantum chemical parameters obtained by DFT analysis suggest that the Glutamic acid adsorb on the steel surface through active centers identified in this compound and the results are in well agreement with experimental findings.

References

- [1] S. Issaadi, T. Douadi, and S. Chafaa, *Appl. Surf. Sci.* 316(2014)582-589.
- [2] X. Zheng, M. Gong, and C. Liu, *Int. J. Electrochem. Sci.* 12(2017) 5553-5566
- [3] R.T. Loto, *Revista Colombiana de Química.* 47(2018)12-20.
- [4] S. Gowri, J. Sathiyabama, and S. Rajendran, *International Journal of ChemTech Research.* 5(2013)347-352
- [5] M. Mobin, M. Parveen, and M. Khan, *PortugaliaeElectrochimica Acta.* 29(2011) 391-403
- [6] A. Soumoue, Thèse de Doctorat, Ibn Zohr University, Agadir, Morocco, (2017).
- [7] A. Bouchart, M. Rguiti, K. EL Mouaden, A. Albourine, R. Salghi, L. Bazzi, *Appl. J. Envir. Eng. Sci.* 5(2019) 183-192
- [8] K. Raghavachari, *Theor. Chem. Acc.* 103 (2000) 361–363.
- [9] H. Sun, *J. Phys. Chem. B.* 102 (1998) 7338–7364.
- [10] Y. Inada, H. Orita, *J. Comput. Chem.* 29 (2008) 225–232.
- [11] R.S. Mulliken, *J. Chem. Phys.* 23 (1955) 1833–1840.
- [12] N. Kovačević, A. Kokalj, *Corros. Sci.* 53 (2011) 909–921.
- [13] A. Kokalj, *Chem. Phys.* 393 (2012) 1–12.
- [14] R.G. Pearson, *Proc. Natl. Acad. Sci.* 83 (1986) 8440–8441.
- [15] R.G. Pearson, *Inorg. Chem.* 27 (1988) 734–740.
- [16] A. Chaouiki, H. Lgaz, I.-M. Chung, I. Ali, S.L. Gaonkar, K. Bhat, R. Salghi, H. Oudda, M. Khan, *J. Mol. Liq.* 266 (2018) 603–616.
- [17] A. Dutta, S.K. Saha, P. Banerjee, D. Sukul, *Corros. Sci.* 98 (2015) 541–550.
- [18] C. Verma, L.O. Olasunkanmi, T.W. Quadri, E.-S.M. Sherif, E.E. Ebenso, *J. Phys. Chem. C.* 122 (2018) 11870–11882.
- [19] G. N. Mu, X. Li, & F. Li, *Materials Chemistry and Physics.* 86(1) (2004) 59–68.
- [20] A. Kokalj, *Electrochimica Acta.* 56 (2010) 745–755.
- [21] V. Sastri, J. Perumareddi, *Corrosion.* 53 (1997) 617–622.
- [22] H. Lgaz, S. K. Saha, A. Chaouiki, K. S. Bhat, R., Salghi, P. Banerjee, I.-M. Chung, *Construction and Building Materials,* 233(2020)117320.
- [23] S. K. Shukla & M. Quraishi, *Corros. Sci.* 51(9)(2009)1990–1997.
- [24] H. Lgaz, R. Salghi, S. Jodeh, & B. Hammouti, *J. Mol. Liq.* 225(2017)271–280.
- [25] S. Hu, J. Hu, C. Fan, X. Jia, J. Zhang, & W. Guo, *Acta Chim Sinica.* 68(2010)2051–2058.
- [26] A. Chaouiki, M. Chafiq, H. Lgaz, Shubhalaxmi, K. K. Bhat, I. H. Ali, S. Masroor, Y. El Aoufir, *Appl. J. Envir. Eng. Sci.* 6 (2020) 79-93
- [27] M. Ameer and A. Fekry, *Progress in Organic Coatings.* 71(2011)343-349
- [28] M. Mobin, M. Parveen and M. Khan, *Recent Research in Science and Technology.* 3(2011)40-45.
- [29] W. Yang, W.J. Mortier, *J. Am. Chem. Soc.* 108 (1986) 5708–5711.
- [30] I. Obot, N. Obi-Egbedi, E. Ebenso, A. Afolabi, E. Oguzie, *Res. Chem. Intermed.* 39 (2013) 1927–1948.
- [31] S.K. Saha, A. Dutta, P. Ghosh, D. Sukul, P. Banerjee, *Phys. Chem. Chem. Phys.* 18 (2016) 17898–17911.
- [32] L. Guo, I.B. Obot, X. Zheng, X. Shen, Y. Qiang, S. Kaya, C. Kaya, *Appl. Surf. Sci.* 406 (2017) 301–306.
- [33] R.S. Mulliken, *J. Chem. Phys.* 23 (1955) 1833–1840.
- [34] J.-P. Hansen, I.R. McDonald, *Theory of Simple Liquids: With Applications to Soft Matter*, Academic Press, (2013).